ORIGINAL ARTICLE OPEN ACCESS

Genetic Characterization of a Novel Retron Element Isolated from *Vibrio mimicus*

Jant Cres Caigoy[1] | Toshi Shimamoto[1] | Yojiro Ishida[2] | Ashraf M. Ahmed[3] | Shin-ichi Miyoshi[4,5] | Tadashi Shimamoto[1]

[1]Laboratory of Food Microbiology and Hygiene, Graduate School of Integrated Sciences for Life, Hiroshima University, Higashi-Hiroshima, Japan | [2]Department of Structural Biology, Protein Technologies Center, St. Jude Children's Research Hospital, Memphis, Tennessee, USA | [3]Department of Bacteriology, Mycology and Immunology, Faculty of Veterinary Medicine, Kafrelsheikh University, Kafr El-Sheikh, Egypt | [4]Graduate School of Medicine Dentistry and Pharmaceutical Sciences, School of Pharmaceutical Sciences, Okayama University, Okayama, Japan | [5]Research Center for Intestinal Health Science, Okayama University, Okayama, Japan

Correspondence: Tadashi Shimamoto (tadashis@hiroshima-u.ac.jp)

Received: 6 July 2024 | **Revised:** 3 October 2024 | **Accepted:** 27 October 2024

Funding: This work was supported in part by the Grant-in-Aid for Scientific Research to Tadashi S. from the Japan Society for the Promotion of Science (no. 18K07113, 21K07025).

Keywords: msDNA | retron | reverse transcriptase | *Vibrio mimicus*

ABSTRACT

Bacterial reverse transcriptase coding gene (RT) is essential for the production of a small satellite DNA-RNA complex called multicopy single-stranded DNA (msDNA). In this study, we found a novel retron, retron-Vmi1 (Vm85) from *Vibrio mimicus*. The retron is comprised of the *msr-msd* region, *orf323*, and the *ret* gene, a genetic organization similar to *Salmonella*'s retron-Sen2 (St85). The protein sequence of the RNA-directed DNA polymerase (RT-Vmi1) is highly homologous to the RTs of *Vibrio metoecus, Vibrio parahaemolyticus*, and *Vibrio vulnificus*. Phylogenetic and protein sequence similarity analysis of retron-Vmi1 ORF323 and RT revealed a close relatedness to retron-Sen2. We found that retron-Vmi1 was inserted in the *dusA* gene, similar to the insertion of the retron-Vpa1 (Vp96) of *V. parahaemolyticus* AQ3354, suggesting that retrons can be transferred via the tRNA gene. These results are the first convincing evidence that retron is moving across species. The neighboring genes of retron-Vmi1 shared high homology with the genetic environment of *V. parahaemolyticus* and *V. vulnificus* retrons. We also found two junction points within the retron-Vmi1 and the *dusA* gene suggesting that retron-Vmi1 was inserted into this site in a two-step manner.

1 | Introduction

Retrons are retro-elements that are inserted into the bacterial chromosome or as part of a large prophage DNA element in different bacterial species [1, 2]. Retrons are essential to produce msDNA, a small satellite DNA-RNA complex. The retron is comprised of an *msr* (RNA coding region), *msd* (DNA coding region), and the *ret* (reverse transcriptase, RT) gene [3]. Bacterial RTs have the ability to synthesize both double-strand DNA and single-stranded cDNA [4]. Retrons are speculated as mobile elements according to msDNAs similarities, properties, and amino acid identity of RTs as well as the transposition of retron in the genome [5, 6]. Only one definitive function has been attributed to retrons: their role in phage defense [7–9].

Abbreviations: AAA, ATPases associated with diverse cellular activities; BLAST, Basic Local Alignment Search Tool; CT, cholera toxin; DDBJ, DNA Data Bank of Japan; EAEC, enteroaggregative *Escherichia coli*; ENA, European Nucleotide Archives; EPEC, enteropathogenic *Escherichia coli*; IPTG, isopropyl β-thiogalactoside; msDNA, multicopy single-stranded DNA; ORF, open reading frame; RSL, RNA stem loop; RT, reverse transcriptase; ssR, single stranded RNA.

Jant Cres Caigoy and Toshi Shimamoto contributed equally to this study.

Retron elements associated with phage defense consist of three functional components: the *msr-msd* regions, the *ret* gene, and an effector gene, which encodes a protein responsible for the actual defense mechanism against phages [7].

It is suggested that the distribution of retron in prokaryotes is facilitated by lateral gene transmission as indicated by the difference in the GC content of the retron with the host genome [2]. Horizontal gene transfer and acquisition of foreign DNA is a fundamental process in the evolution of most bacterial species [10]. The acquisition of mobile genetic elements such as plasmids, bacteriophages, transposons, integrative and conjugative elements, and genomic islands allows bacteria to instantly obtain a range of genetic traits that may increase fitness under different environmental conditions [11].

Although widely distributed in prokaryotes, the retrons in the bacteria population of the same species or related species seemed to be uncommon [2]. Nowadays, retrons have been isolated from different pathogenic bacteria such as enteroaggregative *Escherichia coli* (EAEC), a classical enteropathogenic *E. coli* (EPEC), *Klebsiella pneumoniae*, *Salmonella enterica* serovar Typhimurium, and *Vibrio cholerae* [12–17]. As a close relative of *V. cholerae*, *Vibrio mimicus* has been implicated as one of the causative agents of gastroenteritis including other infections [18, 19]. The virulence determinants of *V. mimicus* have not been well characterized, but recently it was shown that some *V. mimicus* strains harbor VPI-1 (TCP) and CTXφ (CTX) and produce multiple toxins, including haemolysin, zonula occludens toxin, a heat-stable enterotoxin, and CT-like toxin [20–24].

In this study, we characterized a novel retron, retron-Vmi1, identified in *V. mimicus*, and provided insights into its genetic organization, evolutionary relationships, and potential mechanisms of interspecies transfer. Our results contribute to a better understanding of retron biology and the dynamics of genetic transfer among bacterial species.

2 | Materials and Methods

2.1 | msDNA Isolation

V. mimicus CS30 (*ctx*+) was used in this study. The strain was grown in Lennox broth (LB) supplemented with 1.5% NaCl (final concentration) at 37°C. msDNA from *V. mimicus* CS30 was isolated by the alkaline lysis method, similar to plasmid extraction, as described previously [13].

2.2 | Labeling and Sequencing of msDNA

The DNA part of msDNA was separated by polyacrylamide gel electrophoresis and purified by electroelution. The DNA part of msDNA was labeled at the 3′ end with [α-^{32}P] dideoxyATP and terminal deoxynucleotidyltransferase and purified by urea/polyacrylamide gel electrophoresis [25].

The DNA sequence of msDNA-Vmi1 (Vm85) was determined by the Maxam-Gillbert method as described previously [26]. Based on the sequence of the msDNA part, the retron region was cloned by inverse PCR, and the nucleotide sequence was then determined. The secondary structure of the msDNA-Vmi1 was predicted using the GENETYX-MAC software [27].

2.3 | DNA Sequencing of Retron Region by Inverse PCR

Chromosomal DNA of *V. mimicus* CS30 was prepared by conventional method and DNA was digested with several restriction enzymes [28]. DNA fragments were ligated by using TaKaRa Ligation kit Ver.2 (Takara, Japan) for self-ligation. We used this DNA as a template for PCR. Amplification reactions were carried out with 100 ng of DNA and PCR reaction mixture containing 100 μM deoxynucleoside triphosphate, 1.5 mM $MgCl_2$, 25 pmol of primers, and 1U of Phusion Hot Start High-Fidelity DNA polymerase (FINNZYMES, Finland) and brought to a final volume of 50 μL using distilled water. Primers were designed based on the msDNA sequence. The PCR cycle included initial denaturation at 98°C for 30 s, followed by 30 cycles of denaturation for 5 s at 98°C, primer annealing for 30 s at 55°C, extension for 3 min at 72°C, and a final extension at 72°C for 7 min. The PCR fragment was then purified from the agarose gel using a QIAquick Gel Extraction Kit (Qiagen KK, Japan). Both DNA strands of the PCR product were sequenced using an ABI automatic DNA sequencer (Model 3730xl; Applied Biosystems).

2.4 | Cloning of Retron-Vmi1

Retron-Vmi1 was amplified with the following reaction mixture: 100 ng of chromosomal DNA, 100 μM deoxynucleoside triphosphate, 1.5 mM $MgCl_2$, 25 pmol of primers (ret-F1, ret-R12) and 1U of Phusion Hot Start High-Fidelity DNA polymerase (FINNZYMES, Finland) with a final volume of 50 μL. Primers were designed to amplify a full-length retron-Vmi1. The PCR cycle included initial denaturation at 98°C for 30 s, followed by 30 cycles of denaturation for 5 s at 98°C, primer annealing for 30 s at 55°C, extension for 1.5 min at 72°C, and a final extension at 72°C for 7 min. The PCR fragment was then purified from the agarose gel using a QIAquick Gel Extraction Kit (Qiagen KK, Japan). Retron-Vmi1 was cloned into *Sma*I-digested pBluescript II SK (-) (Stratagene, USA) using the TaKaRa Ligation Kit Ver.2 (Takara, Japan). Then, the ligation mixtures were used to transform *E. coli* TG1 competent cells. Bacteria were grown in an LB agar medium supplemented with 50 mg/L of X-Gal, 1 mM IPTG, and 100 μg/mL of ampicillin. Positive colonies were screened by a white/blue selection protocol. The recombinant plasmid DNA was isolated from the transformed cells by using a QIAprep Spin Miniprep Kit (Qiagen KK, Japan) and the DNA sequence of the insert was determined for both strands.

2.5 | Genomic Analysis of Retron-Vmi1

The location of retron-Vmi1 from *V. mimicus* CS30 was identified based on the nucleotide sequence of the msDNA-Vmi1.

The *msd* region was determined according to the nucleotide sequence of msDNA-Sen2. The retron promoter was identified based on the conserved promoter sequence using the GENETYX-MAC software. The ORF323 and RT nucleotide similarity search was carried out using the BLAST program (http://www.ncbi.nlm.nih.gov/BLAST/). The *attL* and *attR* sites were located based on the LOGO consensus sequences of *attL* and *attR* direct repeats from *dusA*-specific genome island sequences [28].

To construct the sequence similarity network (SSN), amino acid sequence BLAST of *V. mimicus* ORF323 and RT-Vmi1 was initially performed in the EFI-enzyme similarity tool (EFI-EST) set at UNIPROT BLAST query *e*-value of Log^{-5} [29, 30]. The SSN was then constructed and visualized in Cytoscape 3.10.1 software using the organic layout [31]. Nodes were connected in ORF323 and RT by 45% and 55%, respectively. This was based on the percent similarity with retron-Sen2 ORF320 and RT-Sen2, respectively.

For the phylogenetic analysis, the nucleotide sequence of RT-Vmi1 and representative RTs ($N = 24$) of other bacterial retrons were aligned by ClustalW, and a maximum likelihood phylogenetic tree (1000 bootstrap replicates) [32] was constructed using the MEGA 10.1.8. program [33]. To construct the phylogenetic network, additional RT sequences ($N = 81$) were included and aligned consequently. RT nucleotide sequences were collated using the DnaSP 6.12.03 software resulting to 41 unique RT sequences (considered as RT haplotypes) [34]. The phylogenetic network was then constructed using the TCS method [35] in PopArt 1.7 software [36].

3 | Results and Discussion

3.1 | Identification of msDNA-Vmi1

The DNA part of msDNA was purified from the gel by electroelution after separation by polyacrylamide gel electrophoresis, and then the DNA sequence was determined as described above (DDBJ/EMBL/GenBank Accession No. LC791609). The DNA sequence data showed that the msDNA isolated from *V. mimicus* consists of 85 bases of single-stranded DNA and is, thus, referred to as msDNA-Vmi1 (Figure 1).

According to the common structural features of all msDNAs identified to date and the mechanism of msDNA biosynthesis [24], msDNA-Vmi1 was predicted to be branched out from the guanosine residue (branching G) (Figure 1, red highlight) at the 12th position of the RNA molecule by a unique 2′, 5′-phosphodiester linkage, a distinctive feature essential for the reverse transcriptase-mediated priming [37]. The length of the RNA part of msDNA-Vmi1 was predicted to be 79 bases from the *msr* gene of retron-Vmi1 as determined by the identified conserved a1/a2 inverted repeat sequences (Figure 3). The RNA region is comprised of two RNA stem loops (RSL1 and RSL2), three single-stranded RNA segments (ssRa-c), and a DNA-RNA duplex. Interestingly, the DNA stem structure of msDNA-Vmi1 contained a mismatched base pair in its DNA stem (Figure 1, yellow highlight). msDNAs from other pathogenic bacteria containing mismatched base pairs in their DNA stem-loop

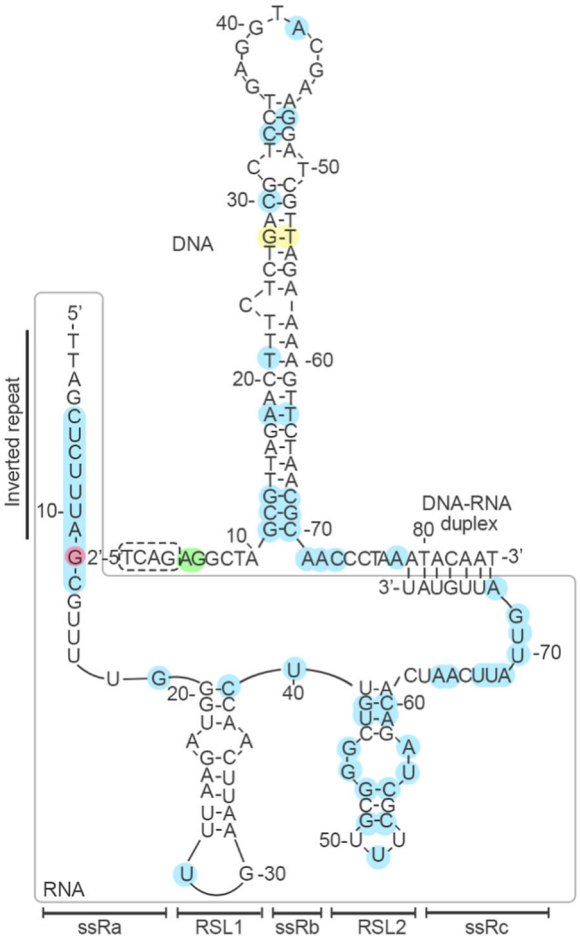

FIGURE 1 | Possible secondary structure of msDNA-Vmi1 from *Vibrio mimicus*. Single-stranded RNA region is boxed, and the branching G residue is highlighted in red. The msDNA cleavage sites are indicated in green highlight, and the mismatch site is in yellow. Conserved regions with other msDNAs.

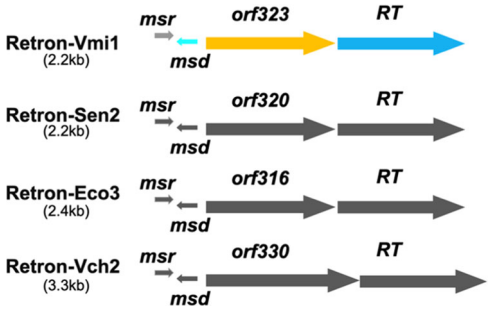

FIGURE 2 | Gene organization of bacterial retrons containing gene encoding for a putative inner membrane protein. The location of the genes and their transcriptional directions are indicated by arrows. The *orf323* of retron-Vmi1 shares significant similarity with the effector toxin RcaT (*orf320*) of retron-Sen2 (Figure 5A).

structure are regarded as potentially mutagenic [38]. By comparing the msDNA-Vmi1 structure with other msDNAs isolated from pathogenic bacteria, we found a number of conserved regions that are present in all msDNAs of these bacteria (Figure 1, blue highlights), especially msDNA-Sen2 from *S.* Typhimurium. Sequence homology search showed that

V. mimicus CS30 *msr-msd* region (msDNA-Vmi1) shares 100% nucleotide homology with *V. vulnificus* msDNA region, 73.7% with msDNA-Sen2 (from *S.* Typhimurium), 64.2% with msDNA-Eco4 (Ec83) (from EAEC), 61.7% with msDNA-Vpa1 (Vp96) (from *V. parahaemolyticus*), 60.5% with msDNA-Eco7 (Ec78) (from EPEC), and 60.4% with msDNA-Vch1 (Vc95) (from *V. cholerae*).

The conserved tetra nucleotides (Figure 1, dotted box) 5′-TAGA-3′ (in msDNA-Sen2, msDNA-Vch1 (Vc95), and msDNA-Vpa1 or 5′-TTGA-3′ (msDNA-Eco4) that plays an important role during recognition and cleavage of msDNA was not found in msDNA-Vmi1 [39]. msDNA-Vmi1 conserved tetra nucleotides 5′-TCAG-3′ was similar to msDNA-Eco1 (Ec85) (Wang et al., 2022). The cleavage site (Figure 1, green highlight) was conserved among the evaluated msDNA [39]. In the msrRNA, the SLR2 and ssRc, reported to exhibit extensive contact with the reverse transcriptase in msDNA-Eco1, were also conserved in the msDNA-Vmi1 [40]. This ssRc together with the DNA-RNA complex is also found to sit in proximity with the reverse transcriptase active site YADD (Figure 7) [40], which is also conserved among the retron-RTs. These common conserved sequences could denote a common evolutionary origin, and it is interesting to examine whether these sequences are associated with pathogenicity.

3.2 | Organization of Retron-Vmi1

The DNA sequence data retrieved from this study revealed a novel retron in *V. mimicus*, designated as retron-Vmi1, the first reported retron element in *V. mimicus*. Retron-Vmi1 is an operon of approximately 2.2 kb consisting of two open reading frames (ORFs), including the RT (Figure 2). A putative inner membrane protein, designated as ORF323, with 323 amino acid residues is present between the RT (RT-Vmi1; 302 aa) and *msr-msd* region. This genetic organization is similar to that reported for *S.* Typhimurium retron-Sen2 [13]. The promoter region prediction of retron-Vmi1 was predicted 6 bp upstream of the *msr–msd* region as it contains well-conserved −35 and −10 regions (Figure 3).

Upstream of retron-Vmi1, there are two unknown ORFs, ORF276 and ORF133, and they have shown high homology to the proteins downstream of retron-Vpa1, ORF114, and ORF279 (Figure 4). Downstream of retron-Vmi1 are three proteins: ORF356 (AAA family ATPase), ORF361 (site-specific integrase), and ORF359 (site-specific integrase), which are homologous to proteins located on the upstream region of retron-Vpa1. The organization of retron-Vmi1 is similar to retron-Eco3 isolated from a clinical isolate of *E. coli* [41], retron-Sen2 from *S. Typhimurium* [12], and retron-Vch2 (Vc81) from a non-O1/non-O139 *V. cholerae*

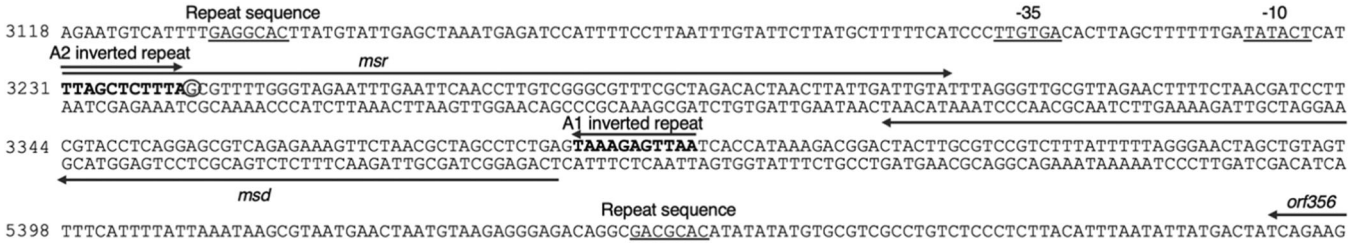

FIGURE 3 | Nucleotide sequence of the upstream and promoter region and the *msr-msd* region of retron-Vmi1. Sequences correspond to the nucleotide region 3118–3456 and 5398–5510 (DDBJ/ENA/GenBank Accession No. LC791609). The second and third lines are shown as double-stranded DNA. The direct repeat region is boldfaced. The predicted promoter sequences (−35 and −10) are underlined. The branching guanosine in the *msr* region is circled. The boldfaced regions indicate the conserved a1/a2 inverted repeat sequences. The underlined sequences indicate the direct repeat sequences.

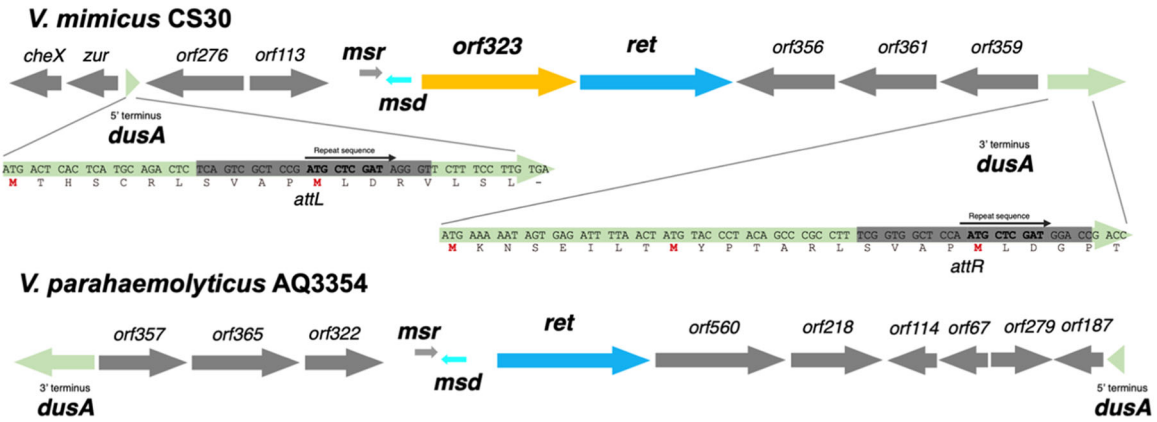

FIGURE 4 | Gene organization of retron-Vmi1 and retron-Vpa1. (A) retron-Vmi1 and its flanking region from *Vibrio mimicus* CS30; (B) retron-Vpa1 and its flanking region from *Vibrio parahaemolyticus* AQ3354.

[42]. These retrons contain an extra ORF between the *msr–msd* region and the *ret* gene (Figure 2).

Amino acid alignment of *V. mimicus* ORF323 with other *Vibrio* spp. showed high similarity with *V. metoecus* (323/323 aa; 100%), *V. cholerae* (322/323 aa; 99.69%), and *V. vulnificus* (316/323 aa; 97.52%). SSN analysis of ORF323 with other bacterial species also revealed that the protein is closely related to the retron-Sen2 family effector protein (Figure 5A). Although the amino acid sequences of these ORFs have significant homology, their associated retrons exist differently on the bacterial chromosome. For example, retron-Eco3 is associated with a prophage, while retron-Sen2 appears to be inserted directly in the chromosome, suggesting that retrons can be inserted in different mechanisms.

3.3 | Comparison of the RT-Vmi1 with the RT from Other Vibrios

We then investigated the homology of RT-Vmi1 to other *Vibrio* spp. and observed 100% identity (301/301 aa) with both *V. metoecus* and *V. parahaemolyticus* and 99.34% (299/301 aa) in *V. vulnificus* (Figure 6).

In addition, we also investigated the homology of RT-Vmi1 with the retron RT of other pathogenic bacteria. The highest similarities to RT-Vmi1 were with RT-Sen2 (from *S.* Typhimurium, 56.5% identity), RT-Vch1 (from *V. cholerae*, 44.5% identity), RT-Eco4 (from aggregative adherence *E. coli*, AAEC, 43.7% identity), RT-Vpa1 (from *V. parahaemolyticus*, 45.4% identity), RT-Eco7 (from enteropathogenic *E. coli*, EPEC, 44.5% identity), and RT-Vch2 (from *V. cholerae*, 46.8% identity). The SSN of RT-Vmi1 exhibits that RT-Vmi1 is more closely related to RT-Sen2 as it is located at the *Salmonella* cluster over the *Vibrio* cluster (Figure 5B).

Multiple amino acid sequence alignments also revealed that these RTs share several highly conserved domains in addition to the highly conserved catalytic tetrad YADD (residues 193–196), the retron-specific region containing the NAXXH (residues 90–94) and VTG triplet (residues 244–246) that are present in all retron RTs (Figure 7) [43, 44]. This suggests that RTs associated with retrons exhibit high sequence similarity when they share similar genetic organization. The high similarity indicates that these RTs are likely to perform similar functions, specifically in the production or regulation of msDNAs in bacteria.

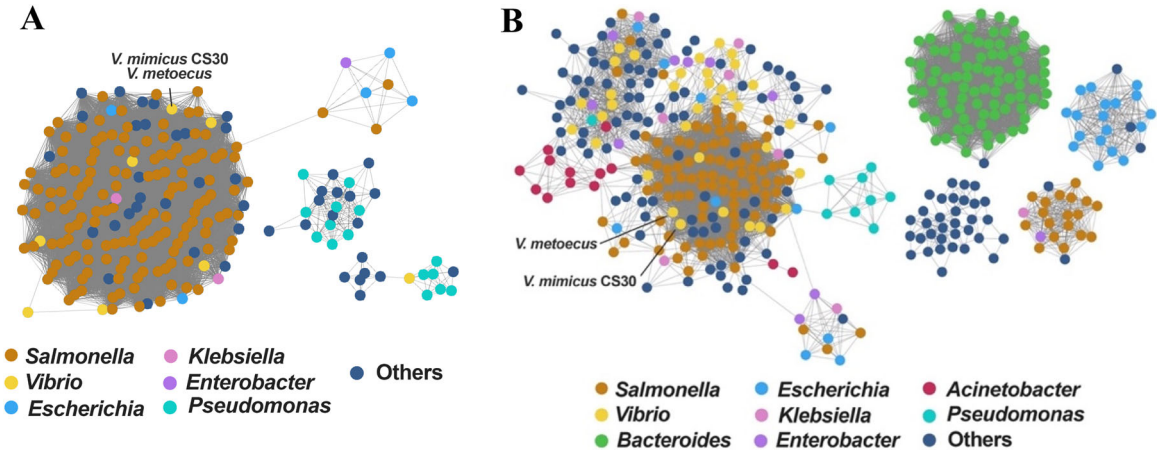

FIGURE 5 | Amino acid sequence similarity network (SSN) of *Vibrio mimicus* CS30 (A) ORF323 and (B) RT. The network was thresholded at a BLAST E-value of 1×10^{-5}. Sequence BLAST and network data were generated using the EFI-EST database, and the SSN was constructed in Cytoscape using an organic layout. The ORF323 full network contains 342 nodes with edges connected at ≥ 45% identity. The RT full network contains 978 nodes with edges connected at ≥ 55% identity.

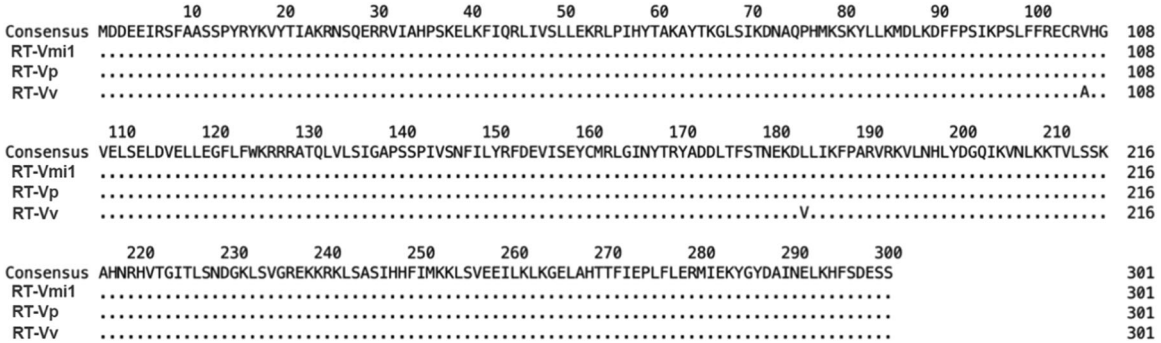

FIGURE 6 | Amino acid alignment of RT-Vmi1 with the RTs from *Vibrio parahaemolyticus* PHLUSAVBR00185 and *Vibrio vulnificus* V252. Similar amino acid residues are denoted by dots.

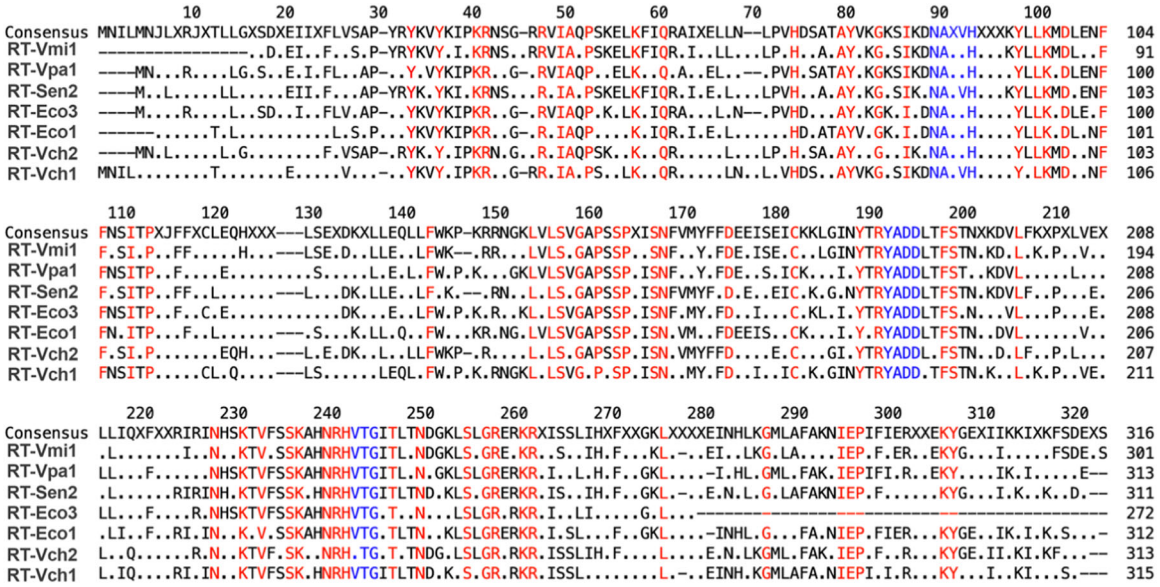

FIGURE 7 | Amino acid alignment of RTs from different bacterial retrons. Conserved amino acid sequences are labeled in red, which includes the YXDD and VTG boxes in blue. Dissimilar sites are denoted by dots.

3.4 | Phylogenetic Analysis of RT-Vmi1

We then carried out a phylogenetic analysis of RT-Vmi1 to determine its genetic lineage. A phylogenetic tree was constructed using the nucleotide sequences of *ret* (RT) genes (Figure 8). The phylogenetic tree analysis showed a significant diversity among the host bacterial species, as RT-Vmi1 of *V. mimicus* associates closely with RT-Sen2 of *S.* Typhimurium rather than the RT-Vch1 of *V. cholerae* and RT-Vpa1 of *V. parahaemolyticus*. The data indicate that several bacterial species, including *E. coli, Salmonella*, and *Vibrio*, have likely acquired the retron very similar to retron-Sen2 through a transduction event. This is evidenced by the related retron-Eco3 (Figure 2), which is still found in a functional prophage DNA. The presence of both *attL* and *attR* sites also suggests that these retrons are associated with prophage DNA sequences (Figure 4). These results substantiate that retrons are indeed mobile genetic elements, which can migrate between different bacterial species. The phylogenic tree showed the RTs from investigated *Vibrio* species split into two subclades, one associated with *E. coli* RTs and one with *Salmonella* Sen2 family RTs. The 1-A retron type under which retron-Eco7, Eco4, Vpa1, and Vch1 belong is characterized by an associated/fused protein domain containing an N-terminal ATPase module [45]. Whereas retron-Sen2, Vch2, and Eco3 (Ec73) contain an N-terminal nucleoside deoxyribosyltransferase-like (NDT) + C-terminal DNA binding domain, a characteristic also shared by retron-Vmi1. It is no surprise that RT-Vmi1 is more closely related to the *V. cholerae* non-O1/non-O139 RT (RT-Vch2) than RT-Vch1 of pathogenic *V. cholerae* (Figure 8). Such observation could provide information on the evolutionary process of *V. mimicus* from *V. cholerae*.

A haplotype network was constructed to get a clearer relationship of RT-Vmi1 with other *ret* genes associated with the retron element. From the representative nucleotide sequences used in the phylogenetic tree construction, we

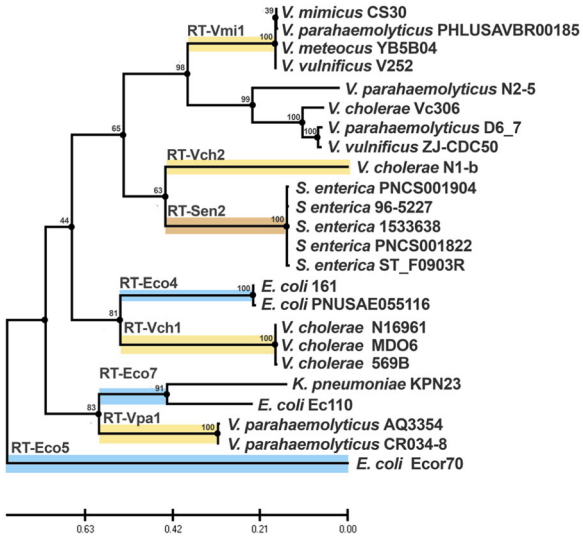

FIGURE 8 | Phylogenetic tree reconstructed based on nucleotide sequences of *ret* (RT) genes (1034 positions). The evolutionary history was inferred using MEGA X with the Maximum Likelihood method and the Tamura-Nei model, yielding the highest log likelihood (−11736.88). The percentage of bootstrap replicates (1000 replicates) supporting each branch is indicated next to the nodes. Branch lengths represent the expected substitutions per site.

have included additional RT sequences to extensively evaluate this genetic relationship. Given that retrons are mobile elements, the TCS network validates that RT-Vmi1 could have descended from *S. enterica* (RT-Sen2) through *V. parahaemolyticus* (Figure 9). The RTs from *V. metoecus* and *V. vulnificus* could have also undergone the same process. Moreover, the RTs from different *Vibrio* species, especially *V. cholerae* and *V. parahaemolyticus*, were scattered throughout the network and did not form a distinct clade indicating that the retron element across different *Vibrio*

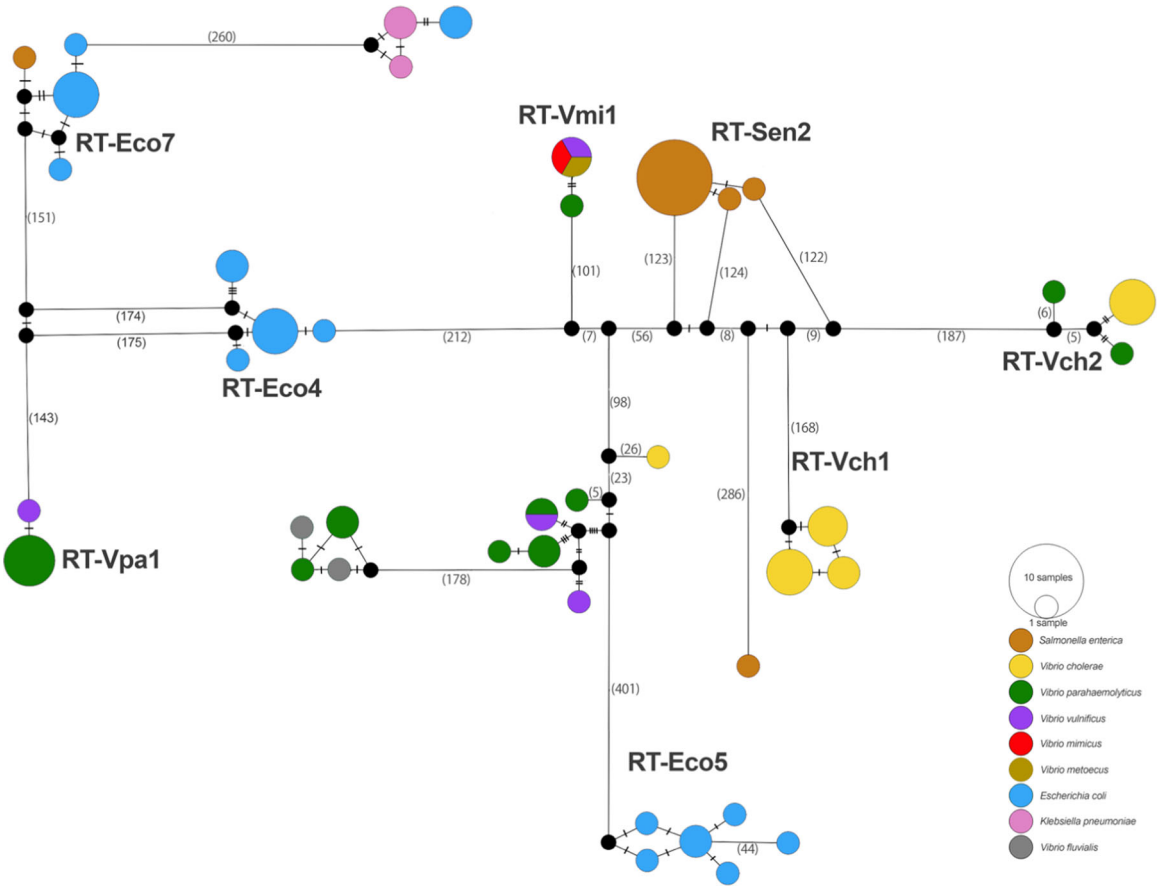

FIGURE 9 | Haplotype network of RT-Vmi1 and other bacterial RT genes constructed using the TCS algorithm [35] in PopArt [36]. The numerical value or the number of dashes between two nodes indicates the number of mutations between nodes. The size of the nodes represents the number of representative samples. Black circles indicate unsampled RT haplotypes.

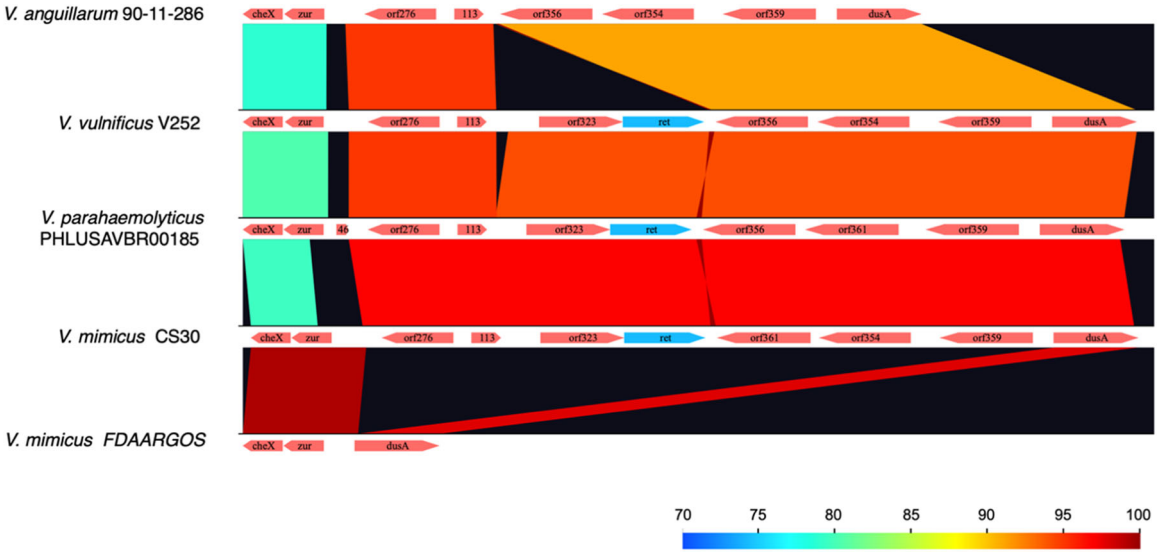

FIGURE 10 | Structure and similarity of retron-Vmi1 and its genomic environment with other *Vibrio* species. The location of the genes and their transcriptional directions are indicated by arrows. This figure is generated using the GenomeMatcher program [47].

species is likely to be more distributed compared to *S. enterica* retrons. This could be attributed to the ubiquity of vibrios in aquatic ecosystems where the mobility of mobile genetic elements, including retrons, is less restricted.

3.5 | Retron-Vmi1 is Inserted into the *dusA* Gene

We further examined the nucleotide sequences upstream and downstream of retron-Vmi1 to find out its insertion environment in

the *V. mimicus* CS30 genome. We found that retron-Vmi1 was inserted into a gene encoding for a tRNA dihydrouridine synthase DusA (*dusA* gene). Interestingly, the retron of *V. parahaemolyticus* AQ3354 (AB433983.1) is also inserted in a similar manner; however, the composition of its operon is different. Retron-Vmi1 resides in the chromosome with two integrase and helicase genes similar to retron-Vpa1. Interestingly, *attL* and *attR* locations flanked by tRNA dihidrouridine synthase gene in retron-Vpa1, and direct repeat are the same as retron-Vmi1. The sequence of the tRNA gene in vibrios is highly conserved, and the presence of horizontal gene transfer mobile elements between *V. mimicus* and *V. cholerae* suggests that retrons can be transferred via the tRNA gene. Many prophage DNAs and other related elements, such as integrative and conjugative elements (ICEs) use the tRNA gene as an insertion site [46]. This provides further evidence that the retron in *Vibrio* may have been acquired through a transduction event.

We then compared the retron-Vmi1 environment with other bacterial strains having an RT with high homology to RT-Vpa1 (Figure 10). We found that *V. mimicus* CS30, *V. parahaemolyticus* PHLUSAVBR00185 (AAXMTX000000000), and *V. vulnificus* V252 (NZ_LIIO01000008) have high homology not only in the retron region but also in the neighboring two integrases and DNA regulatory factors. Retron-Vmi1 is inserted between the *zur* and *dusA* genes and the junction point was speculated. This junction point contains a GAGGCAC sequence which is located upstream of the *msr-msd* region. Surprisingly, we found *V. anguillarum* 90-11-286 (CP011460), which lacks the retron region. Hence, the existence of another junction point (junction point 2) in the retron region was also speculated. This second junction point contains an ATGCTCGAT sequence, which was in the 5′ terminus of the *dusA* gene. Our results suggested that retron-Vmi1 was inserted into this site in a two-step manner.

Acknowledgments

This work was supported in part by a Grant-in-Aid for Scientific Research to Tadashi S. from the Japan Society for the Promotion of Science (no. 18K07113, 21K07025).

Disclosure

The authors have nothing to report.

Conflicts of Interest

The authors declare no conflicts of interest.

Data Availability Statement

Data that support the findings of this study are available from the corresponding author upon reasonable request.

REFERENCES

1. I. Rychlik, A. Sebkova, D. Gregorova, and R. Karpiskova, "Low-Molecular-Weight Plasmid of *Salmonella enterica* Serovar Enteritidis Codes for Retron Reverse Transcriptase and Influences Phage Resistance," *Journal of Bacteriology* 183 (2001): 2852–2858, https://doi.org/10.1128/JB.183.9.2852-2858.2001.

2. B. C. Lampson, M. Inouye, and S. Inouye, "Retrons, msDNA, and the Bacterial Genome," *Cytogenetic and Genome Research* 110 (2005): 491–499, https://doi.org/10.1159/000084982.

3. K. Yamanaka, T. Shimamoto, S. Inouye, and M. Inouye, "Retrons," in *Mobile DNA*II, eds. N. L. Graig, R. Craigie, M. Gellert, and A. M. Lambowitz (Washington: ASM Press, 2002), 784–795.

4. L. Pilousova and I. Rychlik, "Retron Se72 Utilizes a Unique Strategy of the Self-Priming Initiation of Reverse Transcription," *Cellular and Molecular Life Sciences* 68 (2011): 3607–3617, https://doi.org/10.1007/s00018-011-0671-0.

5. A. Moya-Beltrán, M. Gajdosik, C. Rojas-Villalobos, et al., "Influence of Mobile Genetic Elements and Insertion Sequences in Long- and Short-Term Adaptive Processes of *Acidithiobacillus ferrooxidans* Strains," *Scientific Reports* 13 (2023): 10876, https://doi.org/10.1038/s41598-023-37341-4.

6. J. Hwang, D. Y. Ye, G. Y. Jung, and S. Jang, "Mobile Genetic Element-Based Gene Editing and Genome Engineering: Recent Advances and Applications," *Biotechnology Advances* 72 (2024): 108343, https://doi.org/10.1016/j.biotechadv.2024.108343.

7. A. Millman, A. Bernheim, A. Stokar-Avihail, et al., "Bacterial Retrons Function in Anti-Phage Defense," *Cell* 183 (2020): 1551–1561.e12, https://doi.org/10.1016/j.cell.2020.09.065.

8. C. Palka, C. B. Fishman, S. Bhattarai-Kline, S. A. Myers, and S. L. Shipman, "Retron Reverse Transcriptase Termination and Phage Defense are Dependent on Host RNase H1," *Nucleic Acids Research* 50 (2022): 3490–3504, https://doi.org/10.1093/nar/gkac177.

9. J. Bobonis, K. Mitosch, A. Mateus, et al., "Bacterial Retrons Encode Phage-Defending Tripartite Toxin-Antitoxin Systems," *Nature* 609 (2022): 144–150, https://doi.org/10.1038/s41586-022-05091-4.

10. V. Daubin and G. J. Szöllősi, "Horizontal Gene Transfer and the History of Life," *Cold Spring Harbor Perspectives in Biology* 8 (2016): a018036, https://doi.org/10.1101/cshperspect.a018036.

11. D. J. Rankin, E. P. C. Rocha, and S. P. Brown, "What Traits Are Carried on Mobile Genetic Elements, and Why?" *Heredity* 106 (2011): 1–10, https://doi.org/10.1038/hdy.2010.24.

12. S. A. Rice, J. Bieber, J. Y. Chun, G. Stacey, and B. C. Lampson, "Diversity of Retron Elements in a Population of Rhizobia and Other Gram-Negative Bacteria," *Journal of Bacteriology* 175 (1993): 4250–4254, https://doi.org/10.1128/jb.175.13.4250-4254.1993.

13. A. M. Ahmed and T. Shimamoto, "msDNA-St85, a Multicopy Single-Stranded DNA Isolated From *Salmonella enterica* Serovar Typhimurium LT2 With the Genomic Analysis of its Retron," *FEMS Microbiology Letters* 224 (2003): 291–297, https://doi.org/10.1016/S0378-1097(03)00450-6.

14. T. M. O. Lima and D. Lim, "A Novel Retron That Produces RNA-Less msDNA in *Escherichia coli* Using Reverse Transcriptase," *Plasmid* 38 (1997): 25–33, https://doi.org/10.1006/plas.1997.1298.

15. D. Lim, "Structure of Two Retrons of *Escherichia coli* and Their Common Chromosomal Insertion Site," *Molecular Microbiology* 5 (1991): 1863–1872, https://doi.org/10.1111/j.1365-2958.1991.tb00810.x.

16. D. Lim, "Structure and Biosynthesis of Unbranched Multicopy Single-Stranded DNA by Reverse Transcriptase in a Clinical *Eschehchia coli* Isolate," *Molecular Microbiology* 6 (1992): 3531–3542, https://doi.org/10.1111/j.1365-2958.1992.tb01788.x.

17. T. Shimamoto, M. Kobayashi, T. Tsuchiya, et al., "A Retroelement in *Vibrio cholerae*," *Molecular Microbiology* 34 (1999): 631–632, https://doi.org/10.1046/j.1365-2958.1999.01531.x.

18. A. Yang, M. Yassin, and T. Phan, "*Vibrio mimicus* Wound Infection in a Burn Patient," *Radiology Case Reports* 16 (2021): 1348–1351, https://doi.org/10.1016/j.radcr.2021.03.021.

19. E. F. Boyd, K. E. Moyer, L. Shi, and M. K. Waldor, "Infectious CTXΦ and the Vibrio Pathogenicity Island Prophage in *Vibrio mimicus*: Evidence for Recent Horizontal Transfer Between *V. mimicus* and *V. cholerae*," *Infection and Immunity* 68 (2000): 1507–1513, https://doi.org/10.1128/IAI.68.3.1507-1513.2000.

20. L. Shi, S. Miyoshi, M. Hiura, K. Tomochika, T. Shimada, and S. Shinoda, "Detection of Genes Encoding Cholera Toxin (CT), Zonula Occludens Toxin (ZOT), Accessory Cholera Enterotoxin (ACE) and Heat-Stable Enterotoxin (ST) in *Vibrio mimicus* Clinical Strains," *Microbiology and Immunology* 42 (1998): 823–828, https://doi.org/10.1111/j.1348-0421.1998.tb02357.x.

21. N. A. Hasan, C. J. Grim, B. J. Haley, et al., "Comparative Genomics of Clinical and Environmental *Vibrio mimicus*," *Proceedings of the National Academy of Sciences United States of America* 107 (2010): 21134–21139, https://doi.org/10.1073/pnas.1013825107.

22. M. Halder, S. Saha, S. Mookerjee, and A. Palit, "Exploring the Dynamics of Toxigenic Environmental *Vibrio mimicus* and its Comparative Analysis With *Vibrio cholerae* of the Southern Gangetic Delta," *Archives of Microbiology* 204 (2022): 420, https://doi.org/10.1007/s00203-022-03028-z.

23. S. M. Morgado, F. dos Santos Freitas, E. Lourenço da Fonseca, and A. C. P. Vicente, "*Vibrio mimicus* Lineage Carrying Cholera Toxin and *Vibrio* Pathogenicity Island, United States and China," *Emerging Infectious Diseases* 30 (2024): 1729–1732, https://doi.org/10.3201/eid3008.240252.

24. T. Shimamoto, M. Y. Hsu, S. Inouye, and M. Inouye, "Reverse Transcriptases From Bacterial Retrons Require Specific Secondary Structures at the 5'-End of the Template for the cDNA Priming Reaction," *Journal of Biological Chemistry* 268 (1993): 2684–2692.

25. A. M. Maxam and W. Gilbert, "Sequencing End-Labeled DNA With Base-Specific Chemical Cleavages," *Methods Enzymol* 65 (1980): 499–560, https://doi.org/10.1016/s0076-6879(80)65059-9.

26. M. E. Mulligan, D. K. Hawley, R. Entriken, and W. R. McClure, "*Escherichia coli* Promoter Sequences Predict *In Vitro* RNA Polymerase Selectivity," *Nucleic Acids Research* 12 (1984): 789–800, https://doi.org/10.1093/nar/12.1part2.789.

27. T. Yee and M. Inouye, "Reexamination of the Genome Size of Myxobacteria, Including the Use of a New Method for Genome Size Analysis," *Journal of Bacteriology* 145 (1981): 1257–1265, https://doi.org/10.1128/jb.145.3.1257-1265.1981.

28. D. N. Farrugia, L. D. H. Elbourne, B. C. Mabbutt, and I. T. Paulsen, "A Novel Family of Integrases Associated With Prophages and Genomic Islands Integrated Within the tRNA-Dihydrouridine Synthase A (*dusA*) Gene," *Nucleic Acids Research* 43 (2015): 4547–4557, https://doi.org/10.1093/nar/gkv337.

29. R. Zallot, N. Oberg, and J. A. Gerlt, "The EFI Web Resource for Genomic Enzymology Tools: Leveraging Protein, Genome, and Metagenome Databases to Discover Novel Enzymes and Metabolic Pathways," *Biochemistry* 58 (2019): 4169–4182, https://doi.org/10.1021/acs.biochem.9b00735.

30. N. Oberg, R. Zallot, and J. A. Gerlt, "EFI-EST, EFI-GNT, and EFI-CGFP: Enzyme Function Initiative (EFI) Web Resource for Genomic Enzymology Tools," *Journal of Molecular Biology* 435 (2023): 168018, https://doi.org/10.1016/j.jmb.2023.168018.

31. P. Shannon, A. Markiel, O. Ozier, et al., "Cytoscape: A Software Environment for Integrated Models of Biomolecular Interaction Networks," *Genome Research* 13 (2003): 2498–2504, https://doi.org/10.1101/gr.1239303.

32. K. Tamura and M. Nei, "Estimation of the Number of Nucleotide Substitutions in the Control Region of Mitochondrial DNA in Humans and Chimpanzees," *Molecular Biology and Evolution* 10 (1993): 512–526, https://doi.org/10.1093/oxfordjournals.molbev.a040023.

33. S. Kumar, G. Stecher, M. Li, C. Knyaz, and K. Tamura, "MEGA X: Molecular Evolutionary Genetics Analysis Across Computing Platforms," *Molecular Biology and Evolution* 35 (2018): 1547–1549, https://doi.org/10.1093/molbev/msy096.

34. P. Librado and J. Rozas, "DnaSP v5: A Software for Comprehensive Analysis of DNA Polymorphism Data," *Bioinformatics* 25 (2009): 1451–1452, https://doi.org/10.1093/bioinformatics/btp187.

35. M. Clement, D. Posada, and K. A. Crandall, "TCS: A Computer Program to Estimate Gene Genealogies," *Molecular Ecology* 9 (2000): 1657–1659, https://doi.org/10.1046/j.1365-294x.2000.01020.x.

36. J. W. Leigh and D. Bryant, "POPART: Full-Feature Software for Haplotype Network Construction," *Methods in Ecology and Evolution* 6 (2015): 1110–1116.

37. A. Dhundale, B. Lampson, T. Furuichi, M. Inouye, and S. Inouye, "Structure of msDNA From *Myxococcus xanthus*: Evidence for a Long, Self-Annealing RNA Precursor for the Covalently Linked, Branched RNA," *Cell* 51 (1987): 1105–1112, https://doi.org/10.1016/0092-8674(87)90596-4.

38. W. K. Maas, C. Wang, T. Lima, A. Hach, and D. Lim, "Multicopy Single-Stranded DNA of *Escherichia coli* Enhances Mutation and Recombination Frequencies by Titrating MutS Protein," *Molecular Microbiology* 19 (1996): 505–509, https://doi.org/10.1046/j.1365-2958.1996.392921.x.

39. K. Kim, D. Jeong, and D. Lim, "A Mutational Study of the Site-Specific Cleavage of EC83, a Multicopy Single-Stranded DNA (msDNA): Nucleotides at the msDNA Stem Are Important for Its Cleavage," *Journal of Bacteriology* 179 (1997): 6518–6521, https://doi.org/10.1128/jb.179.20.6518-6521.1997.

40. Y. Wang, Z. Guan, C. Wang, et al., "Cryo-EM Structures of *Escherichia coli* Ec86 Retron Complexes Reveal Architecture and Defence Mechanism," *Nature Microbiology* 7 (2022): 1480–1489, https://doi.org/10.1038/s41564-022-01197-7.

41. J. Sun, M. Inouye, and S. Inouye, "Association of a Retroelement With a P4-Like Cryptic Prophage (Retronphage phi R73) Integrated into the Selenocystyl tRNA Gene of *Escherichia coli*," *Journal of Bacteriology* 173 (1991): 4171–4181, https://doi.org/10.1128/jb.173.13.4171-4181.1991.

42. K. Inouye, S. Tanimoto, M. Kamimoto, T. Shimamoto, and T. Shimamoto, "Two Novel Retron Elements Are Replaced With Retron-Vc95 in *Vibrio cholerae*," *Microbiology and Immunology* 55 (2011): 510–513, https://doi.org/10.1111/j.1348-0421.2011.00342.x.

43. S. Inouye, M. Y. Hsu, A. Xu, and M. Inouye, "Highly Specific Recognition of Primer RNA Structures for 2'-OH Priming Reaction by Bacterial Reverse Transcriptases," *Journal of Biological Chemistry* 274 (1999): 31236–31244, https://doi.org/10.1074/jbc.274.44.31236.

44. A. J. Simon, A. D. Ellington, and I. J. Finkelstein, "Retrons and Their Applications in Genome Engineering," *Nucleic Acids Research* 47 (2019): 11007–11019, https://doi.org/10.1093/nar/gkz865.

45. M. R. Mestre, A. González-Delgado, L. I. Gutiérrez-Rus, F. Martínez-Abarca, and N. Toro, "Systematic Prediction of Genes Functionally Associated With Bacterial Retrons and Classification of the Encoded Tripartite Systems," *Nucleic Acids Research* 48 (2020): 12632–12647, https://doi.org/10.1093/nar/gkaa1149.

46. P. H. Oliveira, M. Touchon, J. Cury, and E. P. C. Rocha, "The Chromosomal Organization of Horizontal Gene Transfer in Bacteria," *Nature Communications* 8 (2017): 841, https://doi.org/10.1038/s41467-017-00808-w.

47. Y. Ohtsubo, W. Ikeda-Ohtsubo, Y. Nagata, and M. Tsuda, "GenomeMatcher: A Graphical User Interface for DNA Sequence Comparison," *BMC Bioinformatics* 9 (2008): 376, https://doi.org/10.1186/1471-2105-9-376.